Applied Mathematics & Information Sciences
An International Journal

http://dx.doi.org/10.12785/amis/090611

Squeezed Versus Non-Gaussian Fluctuations in Resonance Fluorescence

Héctor M. Castro-Beltrán[1,*], *Luis Gutiérrez*[1] *and Levente Horvath*[2]

[1] Centro de Investigación en Ingeniería y Ciencias Aplicadas, Universidad Autónoma del Estado de Morelos, Avenida Universidad 1001, 62209 Cuernavaca, Morelos, México
[2] Centre for Quantum Science and Technology, Macquarie University, Sydney, NSW 2109, Australia

Received: 11 Feb. 2015, Revised: 11 Apr. 2015, Accepted: 12 Apr. 2015
Published online: 1 Nov. 2015

Abstract: We study theoretically the fluorescence of a two-level atom driven by a laser of weak to moderate intensity, that is, a regime where squeezing would occur. Close to saturation atomic fluctuations dominate and become non-Gaussian, degrading the squeezing. Using Bloch equations and quantum jump trajectories we find that allowing a moderate degree of non-linearity, conditional homodyne detection [G.T. Foster, L.A. Orozco, H.M. Castro-Beltran, H.J. Carmichael, Phys. Rev. Lett. **85**, pp. 3149-3152, 2000] would actually help in observing the elusive squeezing in the fluorescence by increasing the size of the characteristic negative spectrum.

Keywords: Resonance fluorescence, squeezing, non-Gaussian fluctuations

1 Introduction

Squeezing is the quantum effect where fluctuations in one quadrature of the electromagnetic field are reduced below those of a coherent state at the expense of increasing fluctuations in the other quadrature. Squeezed light is efficiently produced by nonlinear effects such as four-wave mixing in optical fibers and optical parametric oscillation [1]. However, squeezing of the resonance fluorescence of a laser driven two-level atom [2,3] is yet to be observed. It would occur in the linear regime, with low laser intensity so that the fluorescence, which itself swamps the squeezing, would be very weak, but the low collection solid angle and non-unit quantum efficiency of detection worsen the prospects for observation. There are proposals to improve the collection efficiency [4] or to enhance the squeezing signal using cavities [5] or feedback [6]. Two experiments succeeded in observing squeezing but in modified conditions: In [7] a long-lived transition is used, little affected by spontaneous emission, and in [8] the atom is strongly coupled to a cavity, where the modal structure surrounding the atom is notably altered.

A different strategy seeks to cancel the effects of detection efficiency [9,10,11,12]. The method of conditional homodyne detection (CHD) has allowed observation of the weakly squeezed light of a cavity QED system [10,11], resulting from single photon fluctuations separated by long time intervals [13]. CHD consists of balanced homodyne measurement of one quadrature conditioned on the detection of a photon from the source, making the measurement free of detector efficiencies. Formally, it is a two-time amplitude-intensity correlation of the source field, giving an expression of *third* order in the field amplitude, thus introducing third order fluctuations. To relate this measurement to squeezing, however, the latter must vanish (if the fluctuations are Gaussian or symmetric about the mean) or must be very small [10,14].

The two-level atom resonance fluorescence has non-Gaussian fluctuations [15]; it is highly non-linear, thus it cannot be described by a quasi-probability distribution. Also, the fourth order moment of the dipole cannot be written in terms of a second order moment, as Gaussians do: the former vanish while the latter is the intensity. Third order fluctuations of resonance fluorescence have already been studied [9,16], but only indirectly, buried in a fourth order (intensity-intensity) correlation.

In this paper we find advantageous to use CHD to reveal non-Gaussianity of fluctuations in resonance fluorescence. Indeed, we find useful to bypass the

* Corresponding author e-mail: hcastro@uaem.mx

restriction to the low driving regime by using the non-negligible third order fluctuations to obtain a picture of the difficulty of dealing with the fragile squeezing alone, and a means to obtain a more measurable spectrum: the extra noise, below saturation, also has a single-peaked negative spectrum. Further, analytical tractability of resonance fluorescence helps to illustrate squeezed and non-Gaussian fluctuations in a manner cavity QED cannot do [10,11,13,17]. A Bloch equations approach allows a separation of the correlation into terms of second and third order in the dipole noise operators [18]. We also apply quantum jump theory [19] to simulate the CHD correlation, even though the proper method would combine quantum jumps and quantum diffusion [10,19,20]. This allows for the analytical calculation for the probability that no photon (or one, or two) is emitted in a suitable observation time. In the weak field limit, where clean squeezing is present, the no-photon history approaches very accurately the exact result.

This paper is organized as follows. First, we briefly review two methods of study of resonance fluorescence. Then, we calculate the amplitude-intensity correlation of CHD, followed by the calculation of the fluctuations spectra. Finally, we discuss the results and give conclusions.

2 Theoretical Model

We consider a single two-level atom interacting with a monochromatic laser field. The Hamiltonian in the interaction picture is

$$\mathscr{H} = \hbar\Delta\sigma_+\sigma_- + \frac{\hbar\Omega}{2}(\sigma_+ + \sigma_-)\,, \tag{1}$$

where Δ is the detuning of the laser from the atomic transition frequency, Ω is the Rabi frequency describing the coupling strength between atom and laser, and $\sigma_\pm$ are Pauli pseudospin operators. The atom is also coupled to a reservoir of harmonic oscillators at zero temperature which causes spontaneous emission jumps at the rate γ. For concreteness, in this paper we take $\Delta = 0$, which allows to obtain analytical results, though a comment on finite detuning effects is given at the end of Section 4. We briefly review two approaches to study the atomic dynamics.

2.1 Bloch Equations

The Bloch equations describing the atomic dynamics in a slowly rotating frame are [19]

$$\frac{d}{dt}\langle\tilde{\sigma}_\mp\rangle = \mp i\frac{\Omega}{2}\langle\sigma_z\rangle - \frac{\gamma}{2}\langle\tilde{\sigma}_\mp\rangle\,, \tag{2}$$

$$\frac{d}{dt}\langle\sigma_z\rangle = i\Omega\langle\tilde{\sigma}_+\rangle - i\Omega\langle\tilde{\sigma}_-\rangle - \gamma(\langle\sigma_z\rangle + 1)\,, \tag{3}$$

where $\tilde{\sigma}_\mp(t) = \sigma_\mp e^{\pm i\omega t}$ and ω is the laser frequency. The steady state solutions are

$$\langle\tilde{\sigma}_\mp\rangle_{st} = \pm\frac{iY}{\sqrt{2}(1+Y^2)}\,, \tag{4}$$

$$\langle\sigma_z\rangle_{st} = -\frac{1}{1+Y^2}\,, \tag{5}$$

$$\langle\sigma_+\sigma_-\rangle_{st} = \frac{1}{2}(1+\langle\sigma_z\rangle_{st}) = \frac{Y^2}{2(1+Y^2)}\,, \tag{6}$$

where $Y = \sqrt{2}\,\Omega/\gamma$. Throughout this paper steady state values are denoted with the subindex *st*. For later reference, we replace the atomic operators by its mean plus noise,

$$\sigma_m(t) = \langle\sigma_m\rangle_{st} + \Delta\sigma_m(t)\,, \tag{7}$$

where $m = -,+,z$, leading to the equations

$$\frac{d}{dt}\langle\Delta\tilde{\sigma}_\mp\rangle = \mp i\frac{\Omega}{2}\langle\Delta\sigma_z\rangle - \frac{\gamma}{2}\langle\Delta\tilde{\sigma}_\mp\rangle\,, \tag{8}$$

$$\frac{d}{dt}\langle\Delta\sigma_z\rangle = i\Omega\langle\Delta\tilde{\sigma}_+\rangle - i\Omega\langle\Delta\tilde{\sigma}_-\rangle - \gamma\langle\Delta\sigma_z\rangle\,. \tag{9}$$

2.2 Quantum Jump Method

Alternatively, we can study the quantum dissipative evolution solving stochastic Schrödinger equations, some of which simulate actual measurement strategies [19]. A quantum trajectory is a record of a possible history of the wave function. A large ensemble of histories reproduce the density operator. As sketched in the Introduction, we only consider the direct detection of the emitted photons. Due to dissipation the Schrödinger equation $d|\bar{\Psi}_c(t)\rangle/dt = -(i/\hbar)\mathscr{H}_{\rm eff}|\bar{\Psi}_c(t)\rangle$ describes the non-unitary stochastic evolution of the wave function, with periods of coherent evolution interrupted by spontaneous emissions, governed by the effective non-hermitian Hamiltonian

$$\mathscr{H}_{\rm eff} = \mathscr{H} - i\hbar\frac{\gamma}{2}\sigma_+\sigma_-\,. \tag{10}$$

The wave function $|\bar{\Psi}_c(t)\rangle = \bar{c}_g(t)|g\rangle + \bar{c}_e(t)|e\rangle$ is non-normalized and conditioned on its previous evolution. The solutions for the amplitudes from jump to jump, when the initial conditions $\bar{c}_g(0) = 1$ and $\bar{c}_e(0) = 0$ are repeated, are (with $\Delta = 0$)

$$\bar{c}_g(t) = e^{-(\gamma/4)t}\left[\cosh\kappa t + \frac{\gamma}{4\kappa}\sinh\kappa t\right]\,,$$

$$\bar{c}_e(t) = -i\frac{\Omega}{2\kappa}e^{-(\gamma/4)t}\sinh\kappa t\,, \tag{11}$$

where $2\kappa = \sqrt{(\gamma/2)^2 - \Omega^2}$. The emission of a photon is described by the action of the jump operator $\sqrt{\gamma}\sigma_-$, that resets the wave-function to the ground state, at time t_c,

$$|\bar{\Psi}_c(t_c)\rangle \to \sqrt{\gamma}\sigma_-|\bar{\Psi}_c(t_c)\rangle = \sqrt{\gamma}\bar{c}_e(t_c)|g\rangle\,, \tag{12}$$

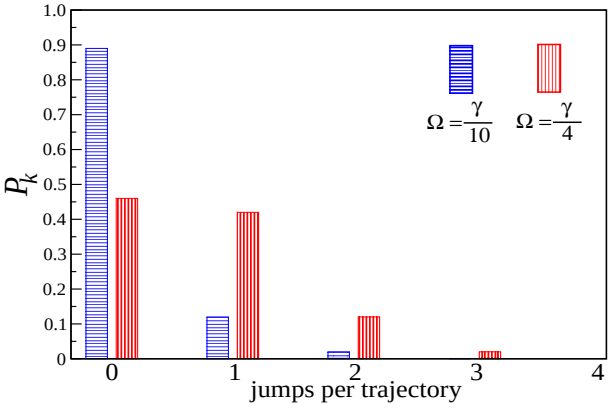

Fig. 1: (Color online) Distribution of the number of jumps per trajectory for an ensemble of 10^5 realizations of length $\gamma T = 15$ and $\Delta = 0$. For weak fields, $\Omega = \gamma/10$, $\overline{k} = 0.12$; at saturation, $\Omega = \gamma/4$, $\overline{k} = 0.68$.

with probability $p_c(t) = \gamma dt \langle \Psi_c | \sigma_+ \sigma_- | \Psi_c \rangle$ in the interval $[t, t+dt]$, where $|\Psi_c(t)\rangle = |\bar{\Psi}_c(t)\rangle / [\langle \bar{\Psi}_c(t) | \bar{\Psi}_c(t) \rangle]^{1/2}$ is the normalized wave function.

Quantum jump trajectories allow to retrieve the photon statistics on the fly [19,21]. Assuming ergodicity, the mean number of photons emitted in the interval $t = [0, T]$ is $\overline{k} = \gamma \int_0^T \langle \sigma_+ \sigma_- \rangle(t) dt$, where T is chosen long enough for the atom-field interaction to have reached the steady state in the ensemble average sense. Figure 1 shows calculations of the probability $P_k(T)$ to have k photons in a trajectory of length T.

Also, one can calculate the average time between two consecutive photons [22],

$$\overline{\tau} = \frac{1}{\gamma \langle \sigma_+ \sigma_- \rangle_{st}} = \frac{\gamma^2 + 2\Omega^2}{\gamma \Omega^2}, \tag{13}$$

where we used Eq. (6). For a propagation time $\gamma T = 15$ we find that for weak driving, $\Omega = \gamma/10$, we have $\gamma \overline{\tau} = 102$, and for moderate driving, $\Omega = \gamma/4$, we have $\gamma \overline{\tau} = 18$. For $\Omega < \gamma/10$, trajectories with $k \geq 2$ events are very rare so, for weak excitation, the weight of one photon events might be obtained approximately by substracting the zero-jump trajectories to the ensemble.

3 Conditional Homodyne Detection

The CHD measures the delayed evolution of a quadrature of the field $E_\phi \propto \sigma_\phi = (1/2)\left(\sigma_- e^{i\phi} + \sigma_+ e^{-i\phi}\right)$ by balanced homodyne detection, where ϕ is the phase between the strong local oscillator and the driving field, conditioned on the direct measurement of the intensity $I \propto \sigma_+ \sigma_-$ at time $\tau = 0$ in the other detector, that is, $\langle I(0) E_\phi(\tau) \rangle$. The normalized third-order correlation in the field amplitude [10,11] is

$$h_\phi(\tau) = \frac{\langle : \sigma_+(0) \sigma_-(0) \sigma_\phi(\tau) : \rangle}{\langle \sigma_+ \sigma_- \rangle_{st} \langle \sigma_\phi \rangle_{st}}, \tag{14}$$

where the dots :: stand for time and normal operator ordering. To calculate $h_\phi(\tau)$ the Bloch equations are solved first and then the quantum regression formula is used [19].

Since $h_\phi(\tau)$ is of odd order in the field amplitude, we expect the CHD to be very sensitive to fluctuations. Indeed, for $\tau \geq 0$ it is the quadrature amplitude of the field that is measured on the cue of a photon count, while for $\tau \leq 0$ it is the intensity that is conditioned on the amplitude measurement. The phase dependence of $h_\phi(\tau)$ makes it non-trivial to relate quadrature amplitude and intensity. For the two-level atom the correlation is given by Eq. (20) below, obtained with a different method in [23,24], which happens to be time-symmetric due to low dimensionality.

To reveal the effects of fluctuations we use Eq. (7) in Eq. (14), thus splitting the amplitude-intensity correlation into correlations of second and third order in the dipole noise operators [18],

$$h_\phi(\tau) = 1 + h_\phi^{(2)}(\tau) + h_\phi^{(3)}(\tau), \tag{15}$$

where

$$h_\phi^{(2)}(\tau) = \frac{2 \langle : \mathrm{Re}[\langle \tilde{\sigma}_- \rangle_{st} \Delta \tilde{\sigma}_+(0)] \Delta \tilde{\sigma}_\phi(\tau) : \rangle}{\langle \sigma_+ \sigma_- \rangle_{st} \langle \tilde{\sigma}_\phi \rangle_{st}}, \tag{16}$$

$$h_\phi^{(3)}(\tau) = \frac{\langle : \Delta \tilde{\sigma}_+(0) \Delta \tilde{\sigma}_-(0) \Delta \tilde{\sigma}_\phi(\tau) : \rangle}{\langle \sigma_+ \sigma_- \rangle_{st} \langle \tilde{\sigma}_\phi \rangle_{st}}. \tag{17}$$

Note that the numerator of Eq. (16) is the autocorrelation of the quadrature fluctuations $\langle : \Delta \tilde{\sigma}_\phi(0) \Delta \tilde{\sigma}_\phi(\tau) : \rangle$, usual in studies of squeezing. Solutions of the two-time correlations are sketched in the Appendix.

The quadrature with $\phi = \pi/2$ is the one that features squeezing, thus most of our results are restricted to this case. The normalization is given by the product of Eq. (6) and $\langle \tilde{\sigma}_{\pi/2} \rangle_{st} = -Y[\sqrt{2}(1+Y^2)]^{-1}$. The CHD correlation for this quadrature is

$$h_{\pi/2}^{(2)}(\tau) = -\frac{1}{1+Y^2} e^{-(3\gamma/4)\tau} \times \left[(1-Y^2) \cosh \delta\tau + \frac{1-5Y^2}{4\delta/\gamma} \sinh \delta\tau \right], \tag{18}$$

$$h_{\pi/2}^{(3)}(\tau) = -\frac{2Y^2}{1+Y^2} e^{-(3\gamma/4)\tau} \times \left[\cosh \delta\tau + \frac{2-Y^2}{4\delta/\gamma} \sinh \delta\tau \right], \tag{19}$$

where $\delta = (\gamma/4)\sqrt{1-8Y^2}$, and the total correlation is

$$h_{\pi/2}(\tau) = 1 - e^{-(3\gamma/4)\tau} \left[\cosh \delta\tau + \frac{1-2Y^2}{4\delta/\gamma} \sinh \delta\tau \right], \tag{20}$$

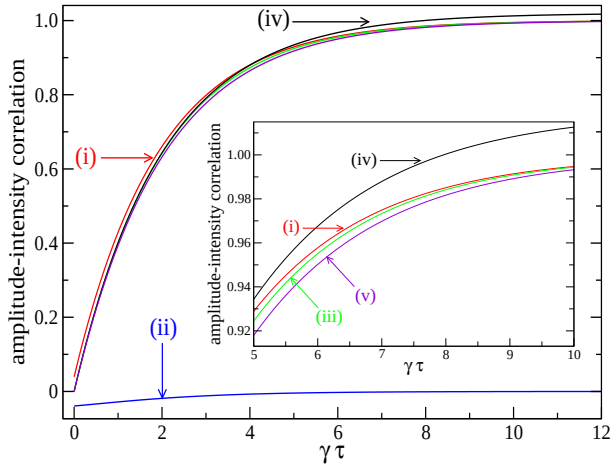

Fig. 2: (Color online) Amplitude-intensity correlation for $\phi = \pi/2$ for weak driving, $\Omega = \gamma/10$. Shown are: (i) $1+h^{(2)}_{\pi/2}$, (ii) $h^{(3)}_{\pi/2}$, (iii) total (exact), (iv) single zero-photon trajectory, and (v) the weak field formula. A large ensemble (not shown) approaches the exact formula.

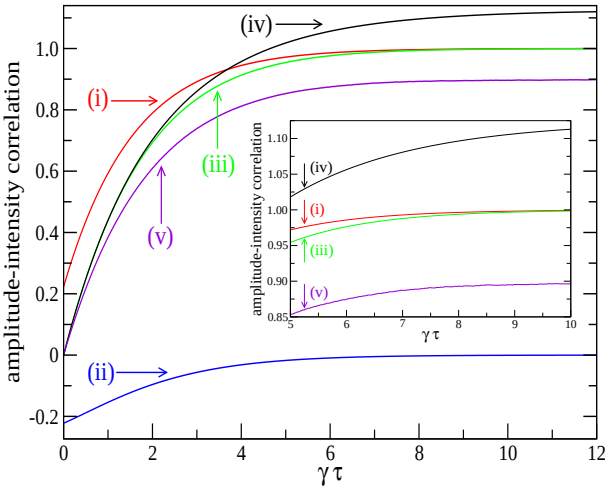

Fig. 3: (Color online) Amplitude-intensity correlation for $\phi = \pi/2$ for driving on saturation, $\Omega = \gamma/4$. Shown are: (i) $1+h^{(2)}_{\pi/2}$, (ii) $h^{(3)}_{\pi/2}$, (iii) total (exact), (iv) single zero-photon trajectory, and (v) a sub-ensemble of zero- and one-photon trajectories. The full ensemble (not shown) contains 10^5 realizations.

with initial values given by

$$h^{(2)}_{\pi/2}(0) = \frac{Y^2-1}{1+Y^2},$$
$$h^{(3)}_{\pi/2}(0) = -\frac{2Y^2}{1+Y^2} = -4\langle\sigma_+\sigma_-\rangle_{st},$$

resulting, from Eq. (15), in $h_{\pi/2}(0) = 0$. For strong driving, $Y^2 \gg 1$, $h^{(3)}_{\pi/2}(0) \to -2$, which implies a large deviation from Gaussian fluctuations.

Special cases are those of the weak field limit, $Y^2 \ll 1$,

$$h^{weak}_{\pi/2}(\tau) = 1 - e^{-(3\gamma/4)\tau}\left[\cosh(\gamma\tau/4) + \sinh(\gamma\tau/4)\right], \tag{21}$$

and at saturation, $\Omega = \gamma/4$ (or $Y^2 = 1/8$),

$$h^{sat}_{\pi/2}(\tau) = 1 - e^{-(3\gamma/4)\tau}\left(1 + \frac{3}{16}\gamma\tau\right). \tag{22}$$

The in-phase quadrature, $\phi = 0$, plays a minor role in this paper. For instance, $\langle\sigma_{\phi=0}\rangle = 0$. Hence, in order to measure a finite signal a coherent offset of amplitude $E_{\rm off}$ has to be added to the source field, modifying Eq. (14) (see [10,18]). This gives

$$h_0(\tau) = 1 + \frac{\langle\sigma_+\sigma_-\rangle_{st}}{\langle\sigma_+\sigma_-\rangle_{st} + E^2_{\rm off}} e^{-\gamma\tau/2}$$
$$= 1 + \left[1 + \frac{(E_{\rm off}Y)^2}{2(1+Y^2)}\right]^{-1} e^{-\gamma\tau/2}. \tag{23}$$

Here $h_0(0) > 1$ and $h^{(3)}_0(\tau)$ is zero at all times.

CHD requires a strong local oscillator field to be mixed with the source's output. The balanced homodyne detection (BHD) arm of the CHD setup thus detects far more photons from the local oscillator than of the source so, strictly, a simulation of the detection process should be of the quantum state diffusion type that, however, keeps a record of the start photons [10]. Our aim, though, is to study the photon emission dynamics and fluctuations near the squeezing conditions. Thus we only use the simpler quantum jump approach to calculate the wave function and, with it, the relevant observables.

It is not possible to split the correlation into terms of second and third order fluctuations when we use quantum trajectory methods. However, with quantum jumps, we may split the correlation into contributions of histories with k photons emitted in a given time interval T,

$$h_\phi(\tau) = \sum_k P_k(T) h_\phi(\tau, k). \tag{24}$$

At $\tau = 0$ we have the *start* photon of the correlation and then count the number of photons k at the *stop* detector in the period T. With each photon emission the atom returns to its ground state.

The $k = 0$ term can be obtained analytically exactly using the solutions (11), which give the evolution of the wave function between two consecutive jumps. Equation

(14) is reduced to $h_\phi(\tau) = \langle\tilde{\sigma}_\phi(\tau)\rangle / \langle\tilde{\sigma}_\phi\rangle_{st}$, where

$$\langle\tilde{\sigma}_\phi(\tau)\rangle = \mathrm{Im}(\bar{c}_e\bar{c}_g^*)/(|\bar{c}_g|^2+|\bar{c}_e|^2) = \frac{(\Omega/2\kappa)\sinh\kappa\tau\,[\cosh\kappa\tau+(\gamma/4\kappa)\sinh\kappa\tau]}{\cosh^2\kappa\tau+\sinh^2\kappa\tau+(\gamma/2\kappa)\cosh\kappa\tau\sinh\kappa\tau} \tag{25}$$

and $\langle\tilde{\sigma}_{\pi/2}\rangle_{st} = -Y[\sqrt{2}(1+Y^2)]^{-1}$. Note that a zero-photon trajectory does not have a steady state but the correlation is normalized with the ensemble value.

Figure 2 shows comparisons of the exact (ensemble), the zero photon ($k=0$) trajectory, the weak field formula, and the second and third order formulas. Figure 3 shows the saturation case, noting that $h_{\pi/2}(\tau)$ needs the $k=0$ and $k=1$ sub-ensembles to approach accurately the exact result (or full ensemble).

It is very important to stress that it is not possible to associate the splittings of Eqs. (15) and (24), on a one to one basis. Even for weak excitation, the no-photon sub-ensemble does not mean that third order fluctuations are absent, or that the one-photon sub-ensemble deviate fluctuations from Gaussian. Even one photon can destroy squeezing.

4 Spectra of Squeezed and other Fluctuations

In most experimental schemes, squeezing is studied in the frequency domain. In CHD the measurement is made in the time domain. This allows to assess the non-classicality of the quadratures, squeezed or not, by the violation of two classical inequalities [18]. The noise spectra of the quadratures are obtained from the Fourier cosine transform of the CHD correlations [10,18]. The spectrum can be split as

$$S_\phi^{(2)}(\omega) = 4\gamma\langle\sigma_+\sigma_-\rangle_{st}\int_0^\infty d\tau\cos(\omega\tau)[h_\phi^{(2)}(\tau)-1], \tag{26}$$

$$S_\phi^{(3)}(\omega) = 4\gamma\langle\sigma_+\sigma_-\rangle_{st}\int_0^\infty d\tau\cos(\omega\tau)h_\phi^{(3)}(\tau). \tag{27}$$

Eq. (26) is a variant of the so-called *spectrum of squeezing*, $S_\phi^{(2)}(\omega) = 2\gamma\int_0^\infty d\tau\cos\omega\tau\langle:\Delta\tilde{\sigma}_\phi(0)\Delta\tilde{\sigma}_\phi(\tau):\rangle$. However, as we will see, the moniker is inaccurate. From Eqs. (18–20,23), we obtain

$$S_0(\omega) = S_0^{(2)}(\omega) = \frac{-2\gamma Y^2}{1+Y^2}\frac{\lambda_0}{\omega^2+\lambda_0^2}, \tag{28}$$

$$S_{\pi/2}^{(2)}(\omega) = \frac{\gamma Y^2}{(1+Y^2)^2}\left[\left(1-Y^2+\frac{1-5Y^2}{4\delta/\gamma}\right)\frac{\lambda_+}{\omega^2+\lambda_+^2} + \left(1-Y^2-\frac{1-5Y^2}{4\delta/\gamma}\right)\frac{\lambda_-}{\omega^2+\lambda_-^2}\right], \tag{29}$$

$$S_{\pi/2}^{(3)}(\omega) = \frac{2\gamma Y^4}{(1+Y^2)^2}\left[\left(1+\frac{2-Y^2}{4\delta/\gamma}\right)\frac{\lambda_+}{\omega^2+\lambda_+^2} + \left(1-\frac{2-Y^2}{4\delta/\gamma}\right)\frac{\lambda_-}{\omega^2+\lambda_-^2}\right], \tag{30}$$

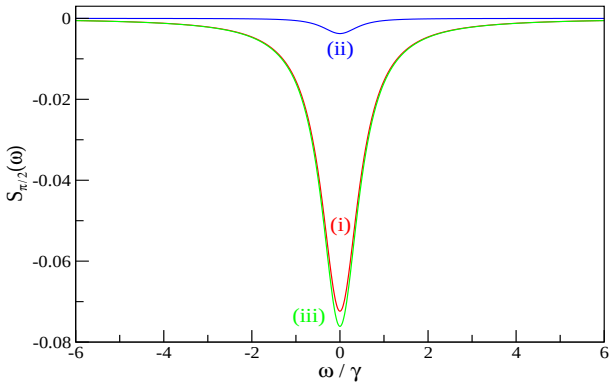

Fig. 4: (Color online) Spectra of fluctuations for $\phi = \pi/2$ for weak driving, $\Omega = \gamma/10$. Shown are the second order (i), third order (ii), and the total spectrum (iii).

where $\lambda_0 = -\gamma/2$ and $\lambda_\pm = -(3/4)\gamma \pm \delta$ [see Eq. (43)]. The total spectrum, $S_{\pi/2}^{(2)}(\omega) + S_{\pi/2}^{(3)}(\omega)$, for $\phi = \pi/2$ is

$$S_{\pi/2}(\omega) = \frac{\gamma Y^2}{1+Y^2}\left[\left(1+\frac{1-2Y^2}{4\delta/\gamma}\right)\frac{\lambda_+}{\omega^2+\lambda_+^2} + \left(1-\frac{1-2Y^2}{4\delta/\gamma}\right)\frac{\lambda_-}{\omega^2+\lambda_-^2}\right]. \tag{31}$$

Let's recall Eqs. (28 –31) are all exact.

$S_0(\omega)$ is a positive Lorentzian of width γ, meaning there is no squeezing for $\phi = 0$, even though $h_0(\tau)$ is non-classical [18]. Moreover, the third order term is zero.

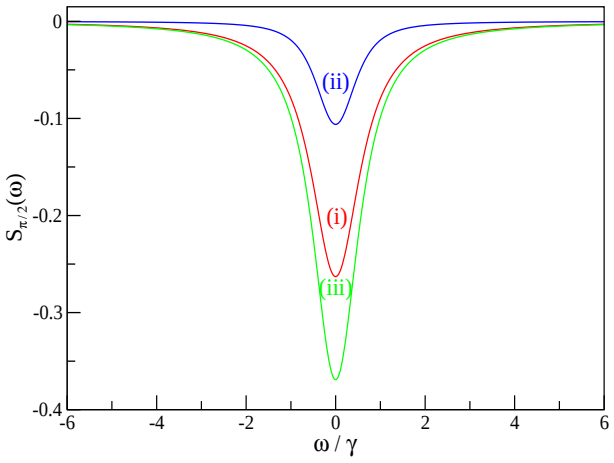

Fig. 5: (Color online) Spectra of fluctuations for $\phi = \pi/2$ for driving on saturation, $\Omega = \gamma/4$. Shown are the second order (i), third order (ii), and the total spectrum (iii).

For the $\phi = \pi/2$ quadrature we emphasize, again, the weak and moderate driving regime. Figures 4 and 5 show

their respective spectra calculated from the exact Eqs. (29-31). The second order term, usually called the spectrum of squeezing, is negative, which indicates that the fluctuations are indeed squeezed. But the third order spectrum is also negative, increasing with the strength of the driving field.

For weak fields, keeping a single Y-dependent correction in Eq. (31) we have

$$S^{weak}_{\pi/2}(\omega) \approx -\gamma^2 Y^2 \left[\frac{1}{\omega^2 + (\gamma/2)^2(1+4Y^2)} + \frac{3\gamma^2 Y^2/2}{[\omega^2 + (\gamma^2/2)(1+Y^2)]^2} \right]. \quad (32)$$

The width of the leading peak is $\gamma(1+2Y^2)$, slightly increased by the presence of the second peak. Disregarding all corrections we find that $S^{weak}_{\pi/2}(\omega) \to -S_0(\omega)$.

Interestingly, Rice and Carmichael [25] found that squeezing reduces the weak field linewidth of the incoherent spectrum of resonance fluorescence, a narrow squared Lorentzian, due to the substraction of two Lorentzians. One of them is slightly smaller but carries the squeezed fluctuations. In the present case, however, the extra noise is correlated to increase the size and width of the spectrum of squeezing.

For saturation intensity, $\Omega = \gamma/4$, we evaluate Eq. (31) at $Y^2 = 1/8$, giving

$$S^{sat}_{\pi/2}(\omega) = -\frac{\gamma^2}{24}\left[\frac{5(3\gamma/4)^2 + 3\omega^2}{[\omega^2 + (3\gamma/4)^2]^2}\right], \quad (33)$$

a squared Lorentzian plus a frequency-dependent term, with linewidth $\Delta\omega = 0.82(3\gamma/2)$. Above saturation the eigenfrequency $\delta = (\gamma/4)\sqrt{1-8Y^2}$ becomes imaginary and sidebands appear.

However, the spectrum remains a single negative peak up to $\Omega \sim \gamma/2$, above which the peak splits. It seems practical then to look at squeezing via the size of the spectrum at the frequency $\omega = 0$,

$$S^{(2)}_{\pi/2}(\omega = 0) = \frac{4Y^2(2Y^2-1)}{(1+Y^2)^3}, \quad (34)$$

$$S^{(3)}_{\pi/2}(\omega = 0) = \frac{2Y^4(Y^2-5)}{(1+Y^2)^3}, \quad (35)$$

$$S_{\pi/2}(\omega = 0) = \frac{2Y^2(Y^2-2)}{(1+Y^2)^2}, \quad (36)$$

shown in Fig. 6, These are negative for $\Omega < \gamma/2$, $\Omega < \gamma\sqrt{5/2}$, and $\Omega < \gamma$, respectively. The minimum of the 2nd order spectrum (maximum squeezing) is seen at $\Omega = 0.3\gamma$. This means that maximal is not optimal, a point observed previously [3,9]. In our case, it means that near and above saturation squeezing might be large but is contaminated by the third order fluctuations. Cleaner squeezing (small third order fluctuations) is limited to $\Omega < 0.1\gamma$.

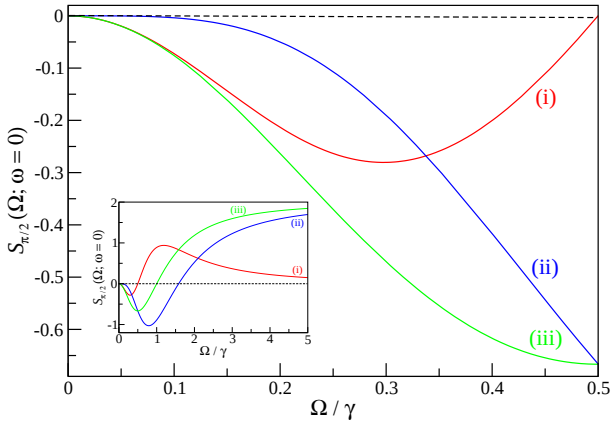

Fig. 6: (Color online) Size of the spectrum at $\omega = 0$ for second order (i), third order(ii), and total (iii) spectrum. For $\Omega > \gamma/2$ (see the inset for an extended range) the total spectrum is no longer a single peak, and for $\Omega > 0.7\gamma$ takes on positive vaues.

4.1 Integrated Spectra and Variances

The integrated spectrum represents the total power emitted by the atom. Likewise, the integrated phase-dependent spectrum represents the size of the noise in a quadrature: in the standard treatment of squeezing it is expressed in terms of the variance, $(4\pi\gamma)^{-1}\int_{-\infty}^{\infty} S^{(2)}_{\phi}(\omega)d\omega = \langle :\Delta\tilde{\sigma}_{\phi}(0)\Delta\tilde{\sigma}_{\phi}(\tau):\rangle = V_{\phi}$ [3]. Integrating Eq. (28) we have

$$\int_{-\infty}^{\infty} S_0(\omega)d\omega = 4\pi\gamma\frac{Y^2}{2(1+Y^2)} = 4\pi\gamma V_0. \quad (37)$$

This is the mean intensity emitted in the full solid angle 4π. Similarly, integrating Eqs. (29) and (30) we have

$$\int_{-\infty}^{\infty} S^{(2)}_{\pi/2}(\omega)d\omega = -4\pi\gamma\frac{Y^2(1-Y^2)}{2(1+Y^2)^2} = 4\pi\gamma V_{\pi/2}, \quad (38)$$

$$\int_{-\infty}^{\infty} S^{(3)}_{\pi/2}(\omega)d\omega = -4\pi\gamma\frac{Y^4}{(1+Y^2)^2}. \quad (39)$$

The former is a well-known result [3], where the variance is negative (i.e., there is squeezing) for $Y^2 < 1$, while the latter is new, negative for all Y, required to match the *total* noise of the in-phase quadrature,

$$\int_{-\infty}^{\infty} S_{\pi/2}(\omega)d\omega = -4\pi\gamma V_0. \quad (40)$$

This is further proof of the non-Gaussianity of resonance fluorescence fluctuations.

4.2 Effect of Finite Detuning

Here we briefly discuss the effect of finite atom-laser frequency detuning on the CHD correlation and spectra.

One should begin with the scattering rate, $\gamma\langle\sigma_+\sigma_-\rangle_{st} = \gamma\Omega^2[2\Omega^2+\gamma^2+4\Delta^2]^{-1}$. The photon rate is reduced with increasing detuning and, hence, the nonlinearity responsible for the third order correlation and spectra. However, the increased generalized Rabi frequency induces oscillations in $h^{(2)}_\phi(\tau)$ at smaller driving intensities, thus the spectrum develops sidebands like those in the strong driving case, with a positive component at $\omega = 0$ [13,18].

5 Discussion and Conclusions

In this paper we have investigated conditions for non-Gaussian fluctuations to manifest in two-level atom resonance fluorescence. Clean squeezing occurs when the atom is very weakly driven, when the average time interval between two consecutive photons is much longer than the regression time to the (ensemble) steady state. In CHD, which is only weakly sensitive to detection inefficiencies, third order fluctuations can be studied naturally. We found it convenient, however, to deviate from the ideal squeezing conditions by considering more moderate laser intensity.

A density operator calculation of the amplitude-intensity correlation allows to split the fluctuations into terms of second and third order in the dipole noise operator. Second order noise is called squeezed if its spectrum is negative. The third order noise increases with the driving intensity in the interval where squeezing occurs, contaminating the latter. Fortunately, for moderately weak driving, both the second and third order fluctuations have coincident negative spectra. This signature of third order fluctuations are more convenient to observe experimentally than looking for clean squeezing in second order correlation measurements.

The quantum jump method makes a decomposition of the CHD correlation in terms of the number of excitations in a measurement time. One has to note, however, that it is not possible, even in the weak field regime, to associate the $k-$th contribution to either the second or the third order dipole fluctuations. One photon is enough to imprint nonlinearity and non-Gaussianity on these fluctuations. The combined analysis, in the framework of conditional homodyne detection, has helped to illustrate the physical processes that lead to the emergence and the degradation of the elusive squeezing in resonance fluorescence.

Finally, the total noise emitted must be independent of the quadrature observed. CHD has permitted us to find the integrated spectrum of the third order fluctuations in the out-of-phase quadrature. The third-order spectrum can be used as a complement to second order spectrum of squeezing to accurately identify and observe the squeezing in the light field emitted by an atom.

Acknowledgement

HMCB thanks Prof. H. J. Carmichael for useful comments and encouragement, and the PIDE program at UAEM for support.

Appendix

We sketch here the analytical solutions of the two-time correlation functions, the numerators of Eqs. (16) and (17), for the dipole fluctuation operators. We start with the Bloch equations for the atomic fluctuations, Eqs. (8) and (9), written compactly as $d\langle\Delta\mathbf{s}\rangle/d\tau = \mathbf{M}\langle\Delta\mathbf{s}\rangle$, where

$$\Delta\mathbf{s} \equiv \begin{pmatrix} \Delta\tilde{\sigma}_- \\ \Delta\tilde{\sigma}_+ \\ \Delta\sigma_z \end{pmatrix}, \qquad \mathbf{M} \equiv \begin{pmatrix} -\gamma/2 & 0 & -i\Omega/2 \\ 0 & -\gamma/2 & i\Omega/2 \\ -i\Omega & i\Omega & -\gamma \end{pmatrix}.$$

Using the quantum regression formula [15], two sets of equations for the correlations of the dipole fluctuation operators, for the second and third order, are then obtained. Both have the structure

$$\frac{d}{d\tau}\langle\Delta\tilde{\sigma}_+(0)\Delta\mathbf{s}(\tau)\Delta A(0)\rangle = \mathbf{M}\langle\Delta\tilde{\sigma}_+(0)\Delta\mathbf{s}(\tau)\Delta A(0)\rangle, \tag{41}$$

with formal solution given by

$$\langle\Delta\tilde{\sigma}_+(0)\Delta\mathbf{s}(\tau)\Delta A(0)\rangle = R^{-1}e^{\lambda\tau}R\langle\Delta\tilde{\sigma}_+\Delta\mathbf{s}\Delta A\rangle, \tag{42}$$

where R is a matrix that diagonalizes $\mathbf{M}$, and $\lambda = \mathrm{diag}(\lambda_0,\lambda_+,\lambda_-)$ is the diagonal matrix of eigenvalues of $\mathbf{M}$ given by

$$\lambda_0 = -\gamma/2, \qquad \lambda_\pm = -(3/4)\gamma \pm \delta. \tag{43}$$

For the second-order correlations, Eq. (16), substitute $\Delta A = \mathbf{1}$ in Eq. (41) with the initial conditions ($\tau = 0$)

$$\langle\Delta\tilde{\sigma}_+\Delta\mathbf{s}\rangle = \begin{pmatrix} \langle\sigma_+\sigma_-\rangle_{st} - |\langle\tilde{\sigma}_+\rangle_{st}|^2 \\ -\langle\tilde{\sigma}_+\rangle^2_{st} \\ -2\langle\tilde{\sigma}_+\rangle_{st}\langle\sigma_+\sigma_-\rangle_{st} \end{pmatrix} = \frac{Y^2/2}{(1+Y^2)^2}\begin{pmatrix} Y^2 \\ 1 \\ i\sqrt{2}Y \end{pmatrix}, \tag{44}$$

leading to the full time-dependent solutions

$$\langle\Delta\tilde{\sigma}_+(0)\Delta\tilde{\sigma}_\mp(\tau)\rangle = \frac{Y^2/4}{1+Y^2}e^{\lambda_0\tau} \mp \frac{Y^2/8}{(1+Y^2)^2} \times \left[\left(1-Y^2+\frac{1-5Y^2}{4\delta/\gamma}\right)e^{\lambda_+\tau} + \left(1-Y^2-\frac{1-5Y^2}{4\delta/\gamma}\right)e^{\lambda_-\tau}\right], \tag{45}$$

$$\langle\Delta\tilde{\sigma}_+(0)\Delta\sigma_z(\tau)\rangle = i\frac{\sqrt{2}Y^3/4}{(1+Y^2)^2}\left[\left(1+\frac{1-2Y^2}{4\delta/\gamma}\right)e^{\lambda_+\tau} + \left(1-\frac{1-2Y^2}{4\delta/\gamma}\right)e^{\lambda_-\tau}\right]. \tag{46}$$

For the third-order correlations, Eq. (17), substitute $\Delta A = \Delta\tilde{\sigma}_-$ in Eq. (41) with the initial conditions

$$\langle \Delta\tilde{\sigma}_+ \Delta \mathbf{s} \Delta\tilde{\sigma}_-\rangle = \begin{pmatrix} 2\langle\tilde{\sigma}_-\rangle_{st}(|\langle\tilde{\sigma}_+\rangle_{st}|^2 - \langle\sigma_+\sigma_-\rangle_{st}) \\ 2\langle\tilde{\sigma}_+\rangle_{st}(|\langle\tilde{\sigma}_+\rangle_{st}|^2 - \langle\sigma_+\sigma_-\rangle_{st}) \\ 2\langle\sigma_+\sigma_-\rangle_{st}(2|\langle\tilde{\sigma}_+\rangle_{st}|^2 - \langle\sigma_+\sigma_-\rangle_{st}) \end{pmatrix} = \frac{Y^4/2}{(1+Y^2)^3}\begin{pmatrix} -i\sqrt{2}Y \\ i\sqrt{2}Y \\ 1-Y^2 \end{pmatrix}, \quad (47)$$

obtaining the time-dependent solutions

$$\langle \Delta\tilde{\sigma}_+(0)\Delta\tilde{\sigma}_\mp(\tau)\Delta\tilde{\sigma}_-(0)\rangle = \mp\frac{iY^5/\sqrt{8}}{(1+Y^2)^3}\left[\left(1+\frac{2-Y^2}{4\delta/\gamma}\right)e^{\lambda_+\tau} + \left(1-\frac{2-Y^2}{4\delta/\gamma}\right)e^{\lambda_-\tau}\right], \quad (48)$$

$$\langle \Delta\tilde{\sigma}_+(0)\Delta\sigma_z(\tau)\Delta\tilde{\sigma}_-(0)\rangle = -\frac{Y^4/4}{(1+Y^2)^3}\left[\left(\frac{1+7Y^2}{4\delta/\gamma}-(1-Y^2)\right)e^{\lambda_+\tau} - \left(\frac{1+7Y^2}{4\delta/\gamma}+(1-Y^2)\right)e^{\lambda_-\tau}\right]. \quad (49)$$

References

[1] H. J. Kimble and D. F. Walls, eds., J. Opt. Soc. Am. B **4**, 1450–1741(1987); R. Loudon and P. L. Knight, eds., J. Mod. Opt. **34**, 709–1020 (1987).
[2] D. F. Walls and P. Zoller, Phys. Rev. Lett. **47**, 709–711 (1981).
[3] M. J. Collett, D. F. Walls, P. Zoller, Opt. Commun. **52**, 145–149 (1984).
[4] M. Stobińska, M. Sondermann, and G. Leuchs, Opt. Commun. **283**, 737–740 (2010).
[5] P. Grünwald and W. Vogel, Phys. Rev. A **88**, 023837 (2013).
[6] A. Barchielli, M. Gregoratti, and M. Licciardo, EPL **85**, 14006.1–6 (2009).
[7] Z. H. Lu, S. Bali, and J. E. Thomas, Phys. Rev. Lett. **81**, 3635–3638 (1998).
[8] A. Ourjoumtsev, A. Kubanek, M. Koch, C. Sames, P. W. H. Pinske, G. Rempe, and K. Murr, Nature **474**, 623 (2011).
[9] W. Vogel, Phys. Rev. Lett. **67**, 2450–2452 (1991); Phys. Rev. A **51**, 4160–4171 (1995).
[10] H. J. Carmichael, H. M. Castro-Beltran, G. T. Foster, and L. A. Orozco, Phys. Rev. Lett. **85**, 1855–1858 (2000).
[11] G. T. Foster, L. A. Orozco, H. M. Castro-Beltran, and H. J. Carmichael, Phys. Rev. Lett. **85**, 3149–3152 (2000).
[12] S. Gerber, D. Rotter, L. Slodička, J. Eschner, H. J. Carmichael, and R. Blatt, Phys. Rev. Lett. **102**, 183601.1–4 (2009).
[13] J. E. Reiner, W. P. Smith, L. A. Orozco, H. J. Carmichael, and P. R. Rice, J. Opt. Soc. Am. B **18**, 1911–1921 (2001).
[14] J. Vines, R. Vyas, and S. Singh, Phys. Rev. A **74**, 023817 (2006).
[15] H. J. Carmichael, Statistical Methods in Quantum Optics 1: Master Equations and Fokker-Planck Equations, Springer-Verlag, Berlin, 1999.
[16] H. J. Carmichael, Phys. Rev. Lett. **55**, 2790–2793 (1985).
[17] A. Denisov, H. M. Castro-Beltran, and H. J. Carmichael, Phys. Rev. Lett. **88**, 243601.1–4 (2002).
[18] H. M. Castro-Beltran, Opt. Commun. **283**, 4680–4684 (2010).
[19] H. J. Carmichael, An Open Systems Approach to Quantum Optics, Springer-Verlag, Berlin, 1993.
[20] H. M. Wiseman and G. J. Milburn, Phys. Rev. A **47**, 1652–1666 (1993).
[21] H. M. Castro-Beltran, E. R. Marquina-Cruz, G. Arroyo-Correa, and A. Denisov, Laser Phys. **18**, 149–156 (2008).
[22] H. J. Carmichael, S. Singh, R. Vyas, and P. R. Rice, Phys. Rev. A **39**, 1200–1218 (1989).
[23] E. R. Marquina-Cruz and H. M. Castro-Beltran, Laser Phys. **18**, 157–164 (2008).
[24] A. Denisov, PhD Thesis (University of Oregon, 2004).
[25] P. R. Rice and H. J. Carmichael, J. Opt. Soc. Am. B **5**, 1661–1668 (1988).
[26] W. Vogel, Phys. Rev. Lett. **100**, 013605.1–4 (2008).

Héctor M. Castro-Beltrán received a Dr. Sc. degree in physics from Instituto Nacional de Astrofísica, Óptica y Electrónica, Mexico, in 1996, where he spent two more years as researcher. From 1998 to 2000 he was Research Associate at University of Oregon, USA. His research interests include quantum optics, cavity QED, laser spectroscopy, open quantum systems, non-stationary optical systems, and quantum information.

Luis Gutiérrez received a Master of Science degree in physics from Universidad Nacional Autónoma de México with a thesis on Wannier-Stark ladders in elastic systems. He is currently working towards a Dr. Sc. degree with Dr. H. M. Castro-Beltrán as advisor. His research interests include quantum optics, laser spectroscopy, and quantum physics analogies in elasticity.

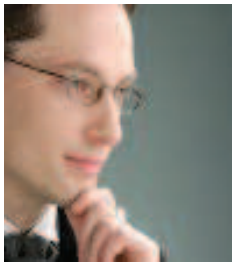

Levente Horvath received a B.Sc. (Hons.) degree and a Ph.D. degree in physics from Macquarie University, Sydney, New South Wales, Australia, in 1996 and 2002, respectively. From 2003 to 2004, he was a Research Associate at Macquarie University working on microwave antennas and waveguides in photonic crystals. He was a Research Fellow at the University of Auckland, Auckland, New Zealand, and the University of Queensland, Brisbane, Queensland, Australia for many years. He is currently a lecturer in Electronic Engineering in Sydney Institute of Business and Technology at Macquarie University. His research interests include quantum optics, cavity QED, quantum information, photonic crystal antennas, stochastic methods, and computational methods for many body problems.